ELSEVIER

Journal of Membrane Science 213 (2003) 195–207

journal of MEMBRANE SCIENCE

www.elsevier.com/locate/memsci

Air-coupled ultrasonic spectroscopy for the study of membrane filters

Tomás E. Gómez Álvarez-Arenas*

Instituto de Acústica CSIC, Serrano 144, 28006 Madrid, Spain

Received 7 June 2002; received in revised form 6 November 2002; accepted 7 November 2002

Abstract

This work presents an investigation carried out to apply a broadband ultrasonic spectroscopy technique to the study of membrane filters. The technique is based on the analysis of the amplitude spectra of broadband airborne ultrasonic pulses transmitted through filter membranes. In particular, analysis of the through thickness resonances is used. Density of the membrane and velocity and attenuation of sound waves are obtained. These magnitudes are correlated to other properties of the membrane like porosity, pore size, water flow and bubble point. Observed relations suggest that this technique can be used as a filter integrity test and as a non-invasive characterization procedure.

Keywords: Ultrasound; Spectroscopy; Membrane characterization; Acoustic velocity and attenuation

1. Introduction

Broadband ultrasonic spectroscopy is a well-known technique used to measure velocity and attenuation of ultrasonic waves in materials. The technique is based on frequency-domain analysis, by using the Fourier transform, of broadband pulses transmitted through a sample, or reflected from it. Density, velocity (or thickness) and attenuation of sound waves and the frequency dependence of these variables can be obtained. In 1978, Sachse and Pao [1] presented an ultrasonic spectroscopy technique, or broadband pulse technique, based on a phase spectral analysis from which phase and group velocity of longitudinal waves can be obtained. Simultaneously, Haines et al. [2] applied broadband ultrasonic spectroscopy to thin layered media. Later, the technique has been improved to measure attenuation, and velocity and attenuation of shear waves [3,4]. Alternatively, Pialucha et al. [5] developed a method to measure phase velocity in plate samples based on the amplitude spectrum instead of phase-spectrum. Compared to time-domain techniques, broadband ultrasonic spectroscopy has many advantages. For example, broadband ultrasonic spectroscopy can be applied to dispersive materials, while time-domain techniques are difficult to apply because of pulse distortion in the time-domain, which is concomitant to dispersive materials. For thin samples or when multiple echoes overlap in the time-domain, it can also be used to determine the velocity of propagation and attenuation.

Recently, a technique called ultrasonic time-domain reflectometry (TDR) has been successfully applied to study filtration membranes [6–10]. In particular, real-time non-invasive measurement of membrane compaction and fouling is studied. An ultrasonic pulse

* Tel.: +34-91-411-76-51; fax: +34-91-561-88-06.
E-mail address: tgomez@ia.cetef.csic.es
(T.E. Gómez Álvarez-Arenas).

0376-7388/02/$ – see front matter
PII: S0376-7388(02)00527-6

reflected on the surface of a membrane is employed. Time-delay measurements are used to determine changes in the membrane due to compaction or fouling. Nevertheless, in some cases, pulses overlap in the time-domain, so direct time-delay measurements are not possible.

Like TDR, main advantage of spectroscopy techniques is that no contact with the sample is required; no contamination is introduced, very rapid inspection is possible as well as on-line and real-time assessment of the status of a membrane. Unlike TDR, ultrasonic spectroscopy provides information not only about one of the surfaces of the membrane but also about the whole volume and the back surface and can be used for precise time-delay measurements even when pulses overlap in the time-domain and when strong dispersion takes place.

Velocity and attenuation of sound in porous materials is closely related to parameters like: pore size, porosity, tortuosity, permeability, and flux resistivity. For example, it is well known that for porous materials like acoustic absorbents flux resistivity can be related to the attenuation of sound waves [11,12]. For some others porous materials [13–16], velocity of slow longitudinal sound waves has been related to pore tortuosity and diffusion and transport properties. Attenuation of sound is very sensitive to the appearance of any external agent in the pore space as moisture [17], and has been used to monitor wetting and drying processes [18]. Velocity of ultrasonic waves have been used in the past to measure elastic coefficient of different kinds of paper [19] and correlate it with properties like tensile breaking strength, compressive strength, etc. Nevertheless, there is no study about the acoustics of membrane filters and the relationship between acoustic and filtration properties.

The purpose of this work is to present the application of an air-coupled ultrasonic broadband spectroscopy technique to the characterization of filtration membranes. In particular, the technique is based on the analysis of the amplitude spectra of broadband ultrasonic pulses transmitted through the membranes. The frequency spectrum of these pulses comprises at least one thickness resonance frequency of the sample under study. The technique can be equally applied to reflected pulses from the membrane. In all cases, density of the membrane and velocity and attenuation of sound waves are obtained. A wide set of commercial membranes is measured and a correlation between acoustical and filtration properties is sought.

In this case wideband and gas-coupled (air-coupled in this work) ultrasound is used. The meaning of this term is two-fold: ultrasonic wideband pulses are transmitted to and received from a gas by gas-coupled transducers and the pulse propagates through a gas gap between sample and transducers. The very high attenuation of ultrasonic waves in the gas phase is a severe problem; this is solved thanks to the use of a new generation of high sensitivity air-coupled piezoelectric transducers that generate ultrasonic broadband pulses at an amplitude high enough to overcome the problem of the attenuation in the gas at the MHz frequency range and ambient pressure [20–22].

Air-coupled ultrasonic spectroscopy has been successfully applied in the past to the characterization of other porous materials like rocks [16], paper [23–25], wood [26], and silica aerogels [27].

2. Materials

A large number of different commercial microporous membranes (23) were used for this study. Different manufacturers, materials, pore sizes, and other filtration properties were selected to have a wide collection of samples; information is gathered in Table 1.

3. Theoretical background

The technique is based on the spectral analysis of broadband ultrasonic pulses transmitted through the samples and the solution of the so-called inverse problem [28]. The situation is schematically depicted in Fig. 1. Transmitter transducer launches an ultrasonic signal; it travels through a gas gap and impinges normally on the surface of the membrane; part of the energy is reflected back while the rest of the energy is transmitted into the membrane. Transmitted wave propagates through the membrane and reaches the back surface; there, part of the energy is reflected back while the rest is transmitted through the interface and received at receiver transducer after traveling through a gas gap. This process is repeated for each of the multiple internal reflections in the membrane. When time-delay between consecutive internal reflections at

Table 1
Main properties of the membranes used for this study

Membrane code	Material	Manufacturer	Porosity (%)	Thickness (μm)	Pore size (μm)	Bubble point (bar)	Water flux at 0.7 bar (ml/(min cm^2))
P-11	Polypropylene	Pall Gelman	NA	125	0.45	1.38	28
P-12	Polypropylene	Pall Gelman	NA	103	0.2	2.9	17
P-2	PVDF	Pall Gelman	NA	133	0.45	1.1	9.6
P-3	Nylon	Pall Gelman	NA	123	0.2	3.8	8
P-41	Polyethersulfone	Pall Gelman	NA	140	0.1	6.9	5
P-42	Polyethersulfone	Pall Gelman	NA	150	0.2	3.2	22
P-43	Polyethersulfone	Pall Gelman	NA	145	0.45	2.1	44
M-11	PVDF	Millipore	NA	112	0.22	NA	15
M-12	PVDF	Millipore	NA	145	0.22	NA	6.9
M-13	PVDF	Millipore	NA	96	0.1	NA	2.5
M-2	PTFE	Millipore	85	100	0.5	0.63	40
M-31	Mixed cellulose esters	Millipore	72	92	0.025	21.1	0.15
M-32	Mixed cellulose esters	Millipore	75	100	0.1	14.1	1.5
M-33	Mixed cellulose esters	Millipore	77	150	0.22	3.52	18
M-34	Mixed cellulose esters	Millipore	79	147	0.45	2.11	60
M-35	Mixed cellulose esters	Millipore	82	168	0.8	1.2	190
M-36	Mixed cellulose esters	Millipore	82	135	1.2	0.77	270
M-37	Mixed cellulose esters	Millipore	83	140	3	0.7	320
M-38	Mixed cellulose esters	Millipore	84	160	5	0.42	580
W-11	Cellulose nitrate	Whatman	66–84	150	0.65	NA	NA
W-12	Cellulose nitrate	Whatman	66–84	135	0.3	NA	NA
W-13	Cellulose nitrate	Whatman	66–84	130	0.2	NA	NA
W-14	Cellulose nitrate	Whatman	66–84	128	0.1	NA	NA

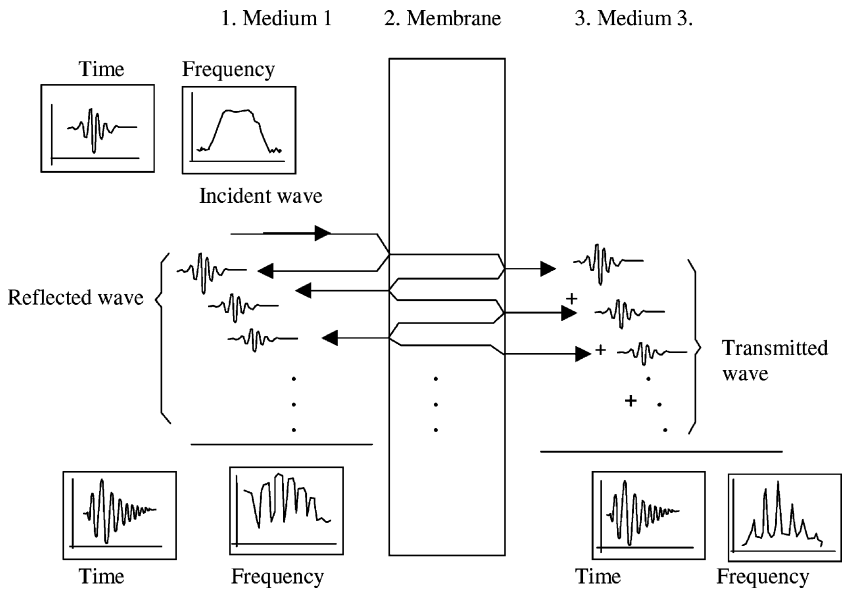

Fig. 1. Schematic illustration of sound transmission through a plate and multiple reverberations within it.

a sample surface equals $1/f$ (being f the frequency of the wave) a constructive interference between multiple reflections within the sample is built up, when this constructive interference takes place at the rear surface of the sample, maximum value of the transmitted energy is observed: this is a thickness resonance of the sample.

Theoretical modeling of the problem of transmission of ultrasonic waves through a membrane separating two media (1 and 3) is carried out considering plane longitudinal waves, normal incidence, and a one-dimensional model. Displacement vector potential can be written in the three space regions (m) denoted as (1, medium 1; 2, membrane filter; 3, medium 3) [29]:

$$\varphi_m = \varphi_m^1 \exp[\mathrm{i}k_m z] + \varphi_m^2 \exp[-\mathrm{i}k_m z], \quad m = 1, 2, 3 \tag{1}$$

where k_m is the wave number in each region of the space, and t the thickness of the membrane. Faces of the membrane are located at $z = 0$ and $z = t$.

Displacement vector u is calculated from the scalar potential φ by:

$$u_m = \mathrm{grad}\,\varphi_m \tag{2}$$

Stress (σ) is calculated from the constitutive equations in each region of the space:

$$\sigma_z^m = c_z^m \frac{\partial u_z^m}{\partial z}, \quad m = 1, 2, 3 \tag{3}$$

where c_z^m are the elastic constant for the z-direction of each space region m.

Stress and displacement must be continuous across membrane surfaces ($z = 0, z = t$). These boundary conditions along with Eqs. (1)–(3) provide a linear system of four equations that can be analytically solved for the coefficients φ_m^i. From these coefficients, displacements, stress, and energy flux in any point of the space can be derived. The transmission coefficient (T) is defined as the ratio of transmitted to incident energy fluxes; a simple analytical expression is obtained:

$$T = \frac{4Z_3(Z_2Z_3)^2}{Z_1[(Z_1Z_2 + Z_3Z_2)^2 \cos^2 \tilde{k}_1 t + (Z_2^2 + Z_1Z_3)^2 \sin^2 \tilde{k}_1 t]} \tag{4}$$

where t is the thickness of the membrane, $\tilde{k}_1$ the complex wave vector in the membrane defined as $\tilde{k}_1 = k_1 - i\alpha_1 = \omega/c_1 - i\alpha_1$, where k_1 is the wave vector, α_1 the longitudinal wave attenuation, c_1 the longitudinal phase velocity, and ω the angular frequency. Z is the specific acoustic impedance, defined as: $Z = c_1\rho$, where ρ is the density, the subindex 1, 2 and 3 refers to medium 1, membrane filter, and medium 3, respectively. When media 1 and 3 have the same acoustic impedance, T is given by:

$$T = \frac{4}{2 + 2\cos^2 \tilde{k}_1 t + ((Z_2^4 + Z_1^4)/Z_2^2 Z_1^2)\sin^2 \tilde{k}_1 t} \tag{5}$$

The employed technique to characterize the membranes is based on experimental measurement and theoretical calculation of the transmission coefficient of ultrasonic waves through membranes. This is done for the frequency range where one or several resonances of the membrane appear. Fitting calculated values of T from Eq. (4) to measured ones provides the velocity of sound in the membrane, the attenuation of sound in the membrane, and the density of the membrane. When media 1 and 3 are the same, we benefit from the simple analytical form of T and all these parameters can be derived in an easy and straightforward way from some simple relations deduced from Eq. (5). In particular, velocity of sound in the membrane is calculated from the measurement of the frequency location of maximum of T, density of the membrane is calculated from minimum value of T, and sound attenuation in the membrane is calculated from the width of the resonance. The procedure is as follows:

(a) *Determination of the velocity of sound in the membrane*: Maximum values of T are located at $kt = n\pi$ ($n = 0, 1, 2, \ldots$). Therefore:

$$f^{(n)} = \frac{nv}{2t} \tag{6}$$

If the thickness of the membrane (t) is known and the frequency where the maximum value of T is located ($f^{(n)}$) is measured, then the velocity of sound in the membrane is calculated from (6). Conversely, if the velocity of sound in the membrane is known, the thickness is worked out. It is worthwhile noting that this result (velocity or thickness) is independent of the properties of the medium surrounding the membrane and to whatever changes may appear in this medium.

(b) *Determination of the density of the membrane*: Minimum values of T are located at $kt = (1/2)n\pi$

($n = 1, 2, \ldots$). From Eq. (5) minimum value of T is given by:

$$T_{\min} = \frac{4Z_2^2 Z_1^2}{(Z_2^2 + Z_1^2)^2} \tag{7}$$

Specific acoustic impedance of the membrane, and hence density, is calculated from the measured minimum value of T and Eq. (7).

(c) *Determination of the attenuation of sound in the membrane*: Q-factor of the resonance observed in the graph T versus frequency (Q) is defined as:

$$Q = \frac{f_r}{\Delta f} \tag{8}$$

where Δf is the width of the resonance peak (T) measured at half-maximum value. Total loss of energy inside the membrane (at resonance) can be calculated from the damping of the resonance peak. It is given by [30]:

$$\tilde{\alpha} = \frac{\pi f_r}{c_1 Q} \tag{9}$$

To obtain the attenuation of sound waves in the membrane (α) it is necessary to consider loss produced by radiation of sound from the membrane. Attenuation is given by:

$$\alpha = \tilde{\alpha} + \frac{\log R^2}{2t} \tag{10}$$

where R is the reflection coefficient at a single membrane/air interface and is defined as ([31], p. 84):

$$R = \frac{(Z_2 - Z_1)^2}{(Z_2 + Z_1)^2} \tag{11}$$

Therefore, from obtained values for the velocity of sound in the membrane (5), the density of the membrane (6), and the measured Q (8), it is possible to work out (Eqs. (9) and (10)) the attenuation of sound in the membrane. In this work, Eqs. (6), (7) and (10) are used to get a first approach to the values of velocity, density and attenuation, these values are entered on a fitting routine to find the values that provide the best agreement (in the sense of least squares) between experimental measurements of T and theoretical results from Eq. (5).

The applicability of this theoretical analysis requires that sample is homogeneous and plate-shaped (surfaces plane and parallel). Plane wave is assumed so that diffraction effects of the sound beam must be negligible. Membranes are porous materials, the application of this theoretical analysis assumes that pore size is much smaller that wavelength so that the two-phase porous media can be replaced by an effective homogeneous media. A more refined approach to the study of wave propagation in porous media is given by Biot's theory [32,33]. This theoretical approach describes sound wave propagation in fluid-saturated porous media. The most interesting result of this approach is the prediction of the appearance of two different longitudinal modes. Sound transmission through and reflection from solid porous plates within the frame of Biot's have also been studied [34–36]. In this work, no evidence is found of the simultaneous propagation of two different longitudinal modes, therefore the effective medium approach is assumed. Nevertheless, it is useful to borrow some of the concepts introduced by Biot's theory to provide a meaningful qualitative explanation of the behavior of the two phases involved in this problem (membrane and air) at a microscopic scale.

4. Experimental set-up

For the experimental work two pairs of specially designed air-coupled piezoelectric transducers were used. They provide enough sensitivity for air-coupled operation and efficient transmission through membranes. They have an operation frequency band that permits the observation of, at least, one resonance for each membrane. These transducers are described in detail in [20–22]. Fig. 2 shows the scheme of the experimental set-up. The two transducers are positioned facing each other and at a distance typically about 2 cm. Transmitter transducer is driven by a high voltage square pulse. It launches an ultrasonic pulse to the air that is picked up and converted into electrical by the receiver transducer; it is amplified up to 110 dB, digitized by an oscilloscope and sent to a computer for storage and further calculations.

First, the signal received through the air gap without the membrane in between is digitized by the oscilloscope and transferred to the computer; the discrete Fourier transform (DFT) is calculated (by a fast Fourier transform (FFT) algorithm). Then the

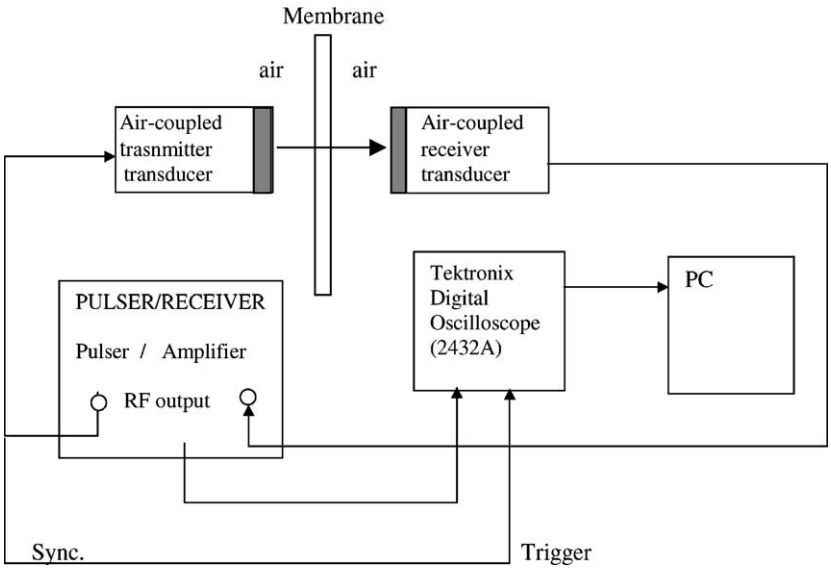

Fig. 2. Schematic representation of the experimental set-up.

Table 2
Experimental results

Membrane code	Density (kg/m^3)	Resonant frequency (f_r, MHz)	Velocity (m/s)	Attenuation at f_r (Np/m)	Attenuation per wavelength
P-11	230	1.4	362.5	2050	0.531
P-12	270	1.82	377	2120	0.439
P-2	500	1.92	515	1200	0.322
P-3	450	1.5	850	800	0.453
P-41	370	2.36	660	445	0.124
P-42	320	1.45	435	335	0.101
P-43	350	1.3	374	460	0.132
M-11	720	1.3	670	1200	0.618
M-12	650	1.1	645	1050	0.616
M-13	800	1.7	750	1000	0.441
M-2		0.3	60	3000	0.600
M-31	700	2	910	440	0.200
M-32	700	1.25	650	440	0.229
M-33	440	1.3	404	650	0.202
M-34	370	1	281	770	0.216
M-35	370	0.75	237	670	0.212
M-36	490	0.82	222	920	0.249
M-37	470	0.86	242	704	0.198
M-38	460	0.68	226	750	0.249
W-11	360	1.3	288	880	0.195
W-12	440	1.6	440	760	0.209
W-13	470	1.94	506	790	0.206
W-14	520	2	508	873	0.222

membrane is put in between the transducers, parallel to transducers faces; received signal is again recorded and FFT calculated. Insertion loss (IL) for the membrane is defined as $IL = 20\log_{10}(A_{sample}/A_{ref})$ where A_{sample} and A_{ref} are the amplitudes of the FFT of recorded waves with and without the membrane in between the transducers, respectively. In this case, coefficient of plane wave transmission through a plate

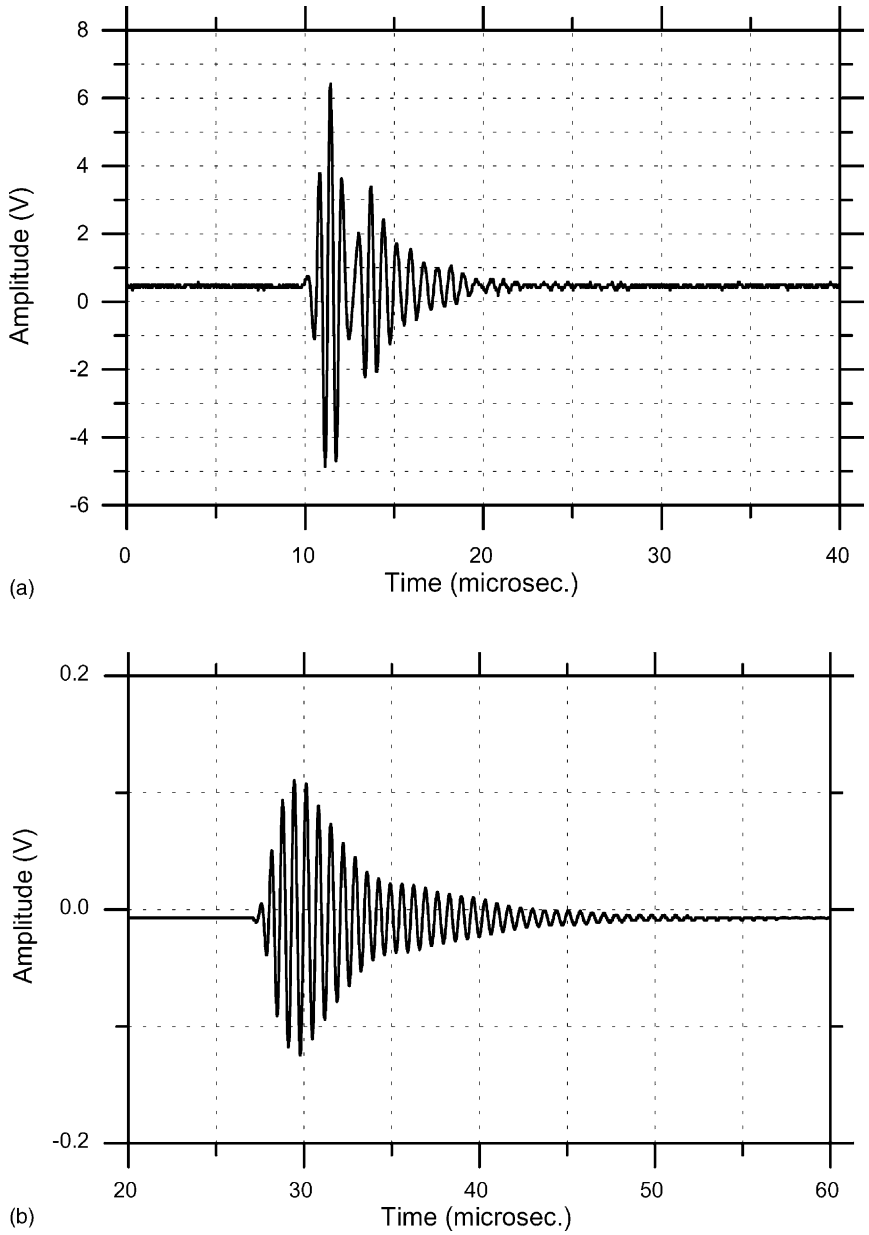

Fig. 3. (a) Transmitted signal through the air gap without the membrane. (b) Transmitted signal with a membrane (polyethersulfone P-41) in between transducers.

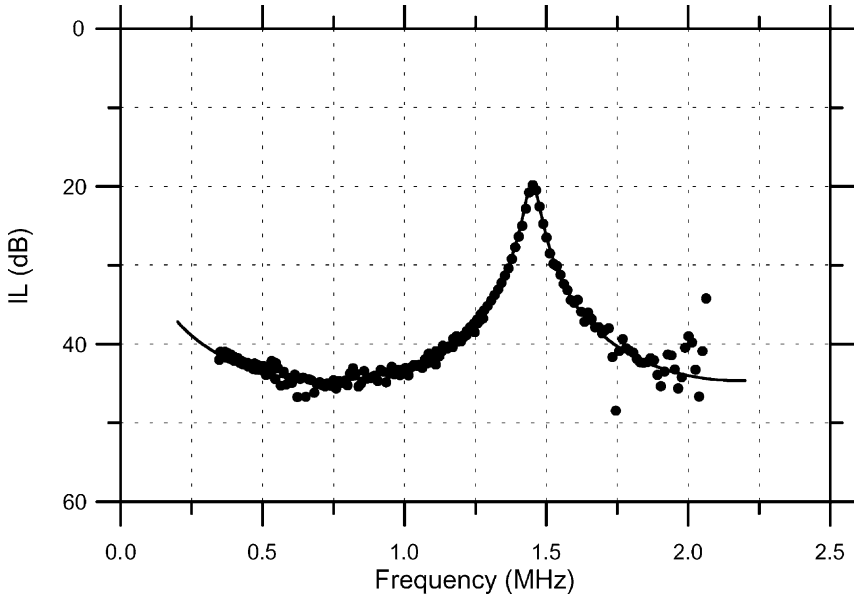

Fig. 4. Insertion loss (dB) vs. frequency corresponding to polyethersulfone membrane P-42 (dots, experimental measurements; solid line, theoretical calculation).

(T) is equal to the ratio of the square of the transmitted pressure amplitude to the square of the incident pressure amplitude ([31], p. 107): $A^2_{\text{sample}}/A^2_{\text{ref}} = T$.

As an example, Fig. 3a and b show the transmitted ultrasonic pulse without and with a membrane (polyethersulfone membrane P-41) in between the transducers, respectively. Fig. 4 shows insertion loss (IL) for the same membrane. Dots are experimental measurements; solid line is the theoretical prediction obtained from Eq. (4) for values of density, velocity and attenuation given in Table 2. The resonance is located at 1.45 MHz; Q-factor of the resonance is 28.

Experimental errors are ± 5 kHz and ± 5 μm for the resonant frequency and the membrane thickness, respectively. This lead to an uncertainty about 5 and 9% for the determination of velocity and attenuation, respectively.

5. Results

Table 2 shows the obtained results for the membranes listed in Table 1. Thickness of each membrane were independently measured. Attenuation per wavelength is also calculated and shown in Table 2. This makes possible a straightforward comparison between attenuation values of different samples.

A first comment to be made is that density and velocity of ultrasonic waves are very low. Similar values have only been reported before for materials like very light paper [24], highly porous PMMA [37], and silica aerogels [25,38].

Fig. 5 shows the plot of the measured velocity of ultrasonic waves versus water flow (ml/(min cm^2) at 0.7 bar). Although data from different membranes made of different materials and by different manufacturers are plotted together, they all seem to follow a common empirical law relating velocity of sound in the membrane and water flow. Velocity changes between two bounds. An upper bound, about 900 m/s, for values of water flow approaching to zero, and a lower bound, about 220 m/s, for samples having very high values of water flow. The major sensitivity of the velocity of sound in the membrane to changes of the water flow are obtained for the range 1–100 (ml/(min cm^2) at 0.7 bar).

A qualitative explanation for this behavior could be given in terms of Biot's theory. At very low values of the water flow, flux resistivity is very high, fluid within the pores is clamped to the solid frame and

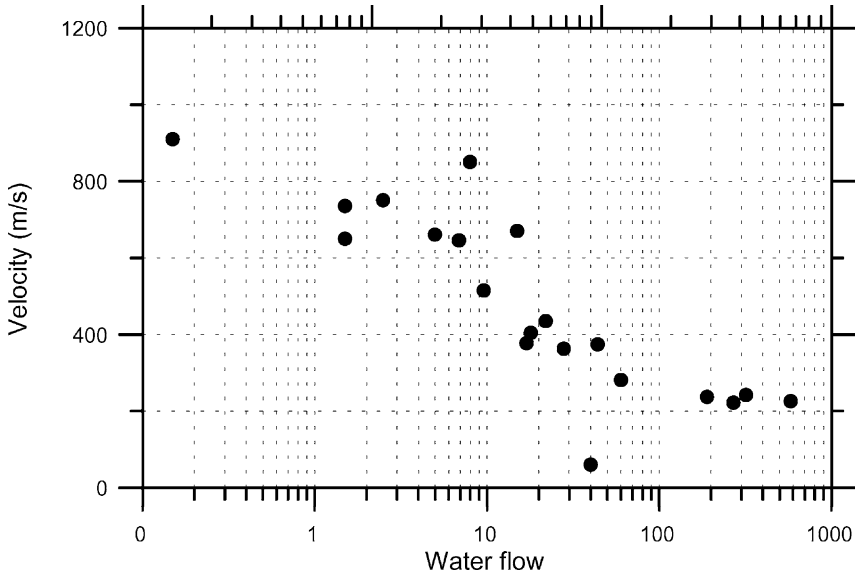

Fig. 5. Measured velocity of ultrasonic waves (m/s) in the membranes vs. water flow (ml/(min cm^2)) measured at 0.7 bar (provided by manufacturers).

the propagation of the acoustic wave takes place moving both phases equally; therefore, most of the acoustic energy is propagated across the solid part of the membrane, and velocity is close to the value observed for bulk polymers (900–2600 m/s). On the contrary, at very high values of water flow, flux resistivity is very low, the fluid in the pores is almost free to move independently of the solid frame under the action of the ultrasonic wave and because of the best matching of acoustic impedances most of the energy propagates through the fluid within the pores [16,39]. In this case, velocity of sound is slightly lower that the velocity in the fluid, in this case air, whose velocity is about 340 m/s. Transition between upper and lower bounds depends on fluid viscosity, pore size, and frequency of the acoustic wave. These two different types of wave propagation are, usually, linked to the fast and slow longitudinal waves predicted by the Biot's theory although no simultaneous propagation of both modes was observed in this case. If the porous frame is much stiffer than the fluid the phase velocity of the slow wave is simply given by [40]:

$$v_{\text{slow}} = \frac{v_{\text{fluid}}}{\sqrt{\alpha}} \tag{12}$$

where α is a factor called tortuosity. For membranes M-34 to M-38 and W-11 it is possible to apply Eq. (12) to get the tortuosity; results are shown in Table 3. Other materials like sintered glass beads and sandstones present tortuosity values in the range 1.7–4 [14,16,35].

It is worthwhile noting that for an air-saturated very soft porous frame it is obtained, in the high frequency limit, that the slow wave velocity approaches to zero while the fast wave velocity is also given by Eq. (12) [41].

A similar dependence is observed between velocity of sound in the membrane and pore size. Results are shown in Fig. 6. Unlike the case analyzed before, now the evolution of the velocity with the pore size is material sensitive. For a given material, for instance mixed

Table 3
Pore tortuosity for some membranes

Membrane code	Velocity (m/s)	Pore tortuosity
M-34	281	1.46
M-35	237	2.05
M-36	222	2.34
M-37	242	1.97
M-38	226	2.26
W-11	288	1.39

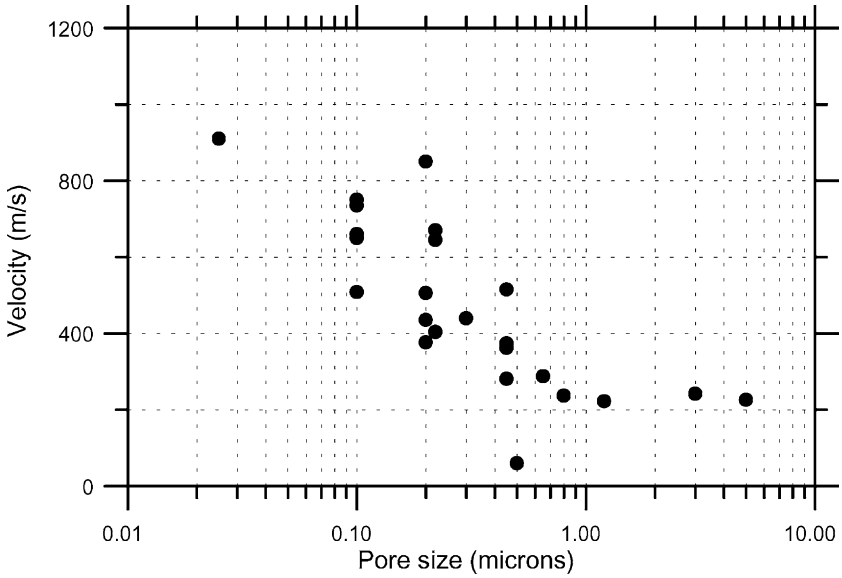

Fig. 6. Measured velocity of ultrasonic waves (m/s) in the membranes vs. pore size (provided by manufacturers).

cellulose esters (M-31 to M-38) velocity decreases gradually as pore size increases. On the contrary, for membranes having the same pore size but made of different materials different velocities are measured. For instance, for pore size 0.2 μm, measured velocity is in the range 850 m/s (nylon membrane P-3) to 377 m/s (polypropylene membrane P-12).

Fig. 7 shows the plot of measured velocity of ultrasonic waves versus bubble point provided by the manufacturers (Table 1). A simple empirical relation

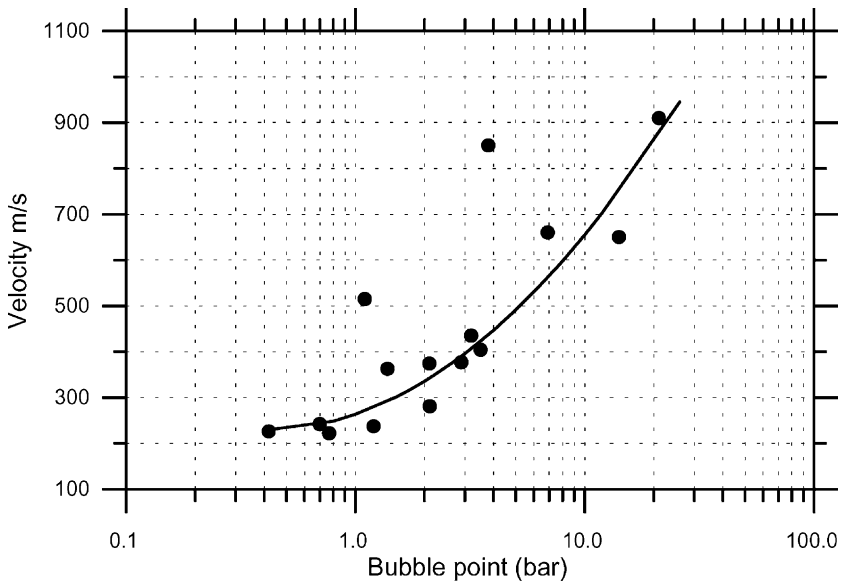

Fig. 7. Measured velocity of ultrasonic waves (m/s) in the membranes vs. bubble point (bar) (provided by manufacturers).

between ultrasonic velocity and bubble point can be deduced:

$$v = 217.6(\log \mathrm{BP} + 0.4)^2 + 228.5 \quad (13)$$

where BP is the bubble point expressed in bar and v the ultrasonic velocity in the membrane in m/s.

Bubble point is commonly used as a non-destructive test to determine the integrity of a membrane filter. The purpose of such a test can be defined [41] as determining "the presence of oversized pores or defects which compromise a given filter's retention capability without destroying the filter". Nevertheless, some authors have pointed out some problems related with this technique: variations up to 10% for the same filter but using different techniques, dependence of the results with filter area, and problems resulting from any damage that can be produced on the filter, when any manipulation is required [42,43].

The close relation between bubble point and the velocity of ultrasonic waves in the membrane suggests that this technique can be used as an alternative or support to bubble point tests. Advantages of the ultrasonic technique is that the measurement procedure is simple, fast and do not require any manipulation of the membrane. Transducers may have a wide aperture (few cm), so that the whole filter surface is measured at once: averaged properties over the filter area are obtained; but it is also possible to use focused transducers to measure the properties of a single point in the membrane ($\sim$1 mm) and to scan the filter surface to measure its properties point by point. Scanning techniques have already been used for other non-destructive purposes and are well known [44].

Concerning attenuation, for cellulose (codes M-3*x* and W-1*x*) and polyethersulfone (code P-4*x*) membranes attenuation per wavelength is independent of pore size, bubble point, and water flow. For other membranes results are not yet determining. On the contrary, as attenuation is very sensitive to membrane fouling, wetting or damage, it can be used to determine the status of a membrane regardless of the grade.

6. Conclusions

A method to characterize porous membranes has been presented. It is based on exciting thickness resonances in the membrane and sensing them. To this end airborne ultrasonic signals generated and received by air-coupled piezoelectric transducers were used. The technique do not require any contact with the membrane, therefore it is non-destructive, non-invasive, clean, and permit a rapid inspection. The measurement of the velocity of ultrasonic waves in the membrane with this technique is not affected by the properties of the surrounding medium or by changes in it. The technique was applied to 23 different membranes. In all cases, the technique is applied successfully and provide a measurement of density and velocity and attenuation of ultrasonic waves in the membrane. These experimental results are compared with other properties of the membranes that are provided by manufacturers: pore size, water flow, and bubble point. For most cases, attenuation per wavelength is independent of pore size, water flow, and bubble point. On the contrary, velocity shows a clear correlation with all these factors; therefore, the use of these two parameters (velocity and attenuation) is a powerful technique to the study of membrane filters. In particular, this technique could be useful to membrane characterization, quality control of membranes, filter integrity tests, on-line assessment of the integrity, fouling, and performance of membranes. Further work is necessary to determine the possibility to use this technique for different experimental and real operation conditions. In addition, some work is still necessary to establish the theoretical background for the observed relation between ultrasonic and filtration properties of a filter membrane.

References

[1] W. Sachse, Y. Pao, On the determination of phase and group velocity of dispersive waves in solids, J. Appl. Phys. 49 (8) (1978) 4320–4327.
[2] N.F. Haines, J.C. Bell, P.J. McIntyre, The application of broadband ultrasonic spectroscopy to the study of layered media, J. Acoust. Soc. Am. 64 (6) (1978) 1645–1651.
[3] R.A. Kline, Measurement of attenuation and dispersion using an ultrasonic spectroscopy technique, J. Acoust. Soc. Am. 76 (2) (1984) 498–504.
[4] J. Wu, Determination of velocity and attenuation of shear waves using ultrasonic spectroscopy, J. Acoust. Soc. Am. 99 (5) (1996) 2871–2875.
[5] T. Pialucha, C.C.H. Guyott, P. Cawley, Amplitude spectrum method for the measurement of phase velocity, Ultrasonics 27 (1989) 270–279.
[6] R.A. Peterson, A.R. Greenberg, L.J. Bond, W.B. Krantz, Use of ultrasonic TDR for real-time non-invasive measurement

of compressive strain during membrane compaction, Desalination 116 (1998) 115–122.
[7] A.P. Mairal, A.R. Greenberg, W.B. Krantz, L.J. Bond, Real-time measurement of inorganic fouling of RO desalination membranes using ultrasonic time-domain reflectometry, J. Membr. Sci. 159 (1999) 185–196.
[8] A.P. Mairal, A.R. Greenberg, W.B. Krantz, Investigation of membrane fouling and cleaning using ultrasonic time-domain reflectometry, Desalination 130 (2000) 45–60.
[9] V.E. Reinsch, A.R. Greenberg, S.S. Kelley, R. Peterson, L.J. Bond, A new technique for the simultaneous, real-time measurement of membrane compaction and performance during exposure to high-pressure gas, J. Membr. Sci. 171 (2000) 217–228.
[10] J. Li, R.D. Sanderson, E.P. Jacobs, Non-invasive visualization of the fouling of microfiltration membranes by ultrasonic time-domain reflectometry, J. Membr. Sci. 201 (2002) 17–29.
[11] M.E. Delany, E.N. Bazley, Acoustical properties of fibrous absorbent materials, Appl. Acoust. 3 (1970) 105–116.
[12] W. Qunli, Empirical relations between acoustical properties and flow resistivity of porous plastic open-cell foam, Appl. Acoust. 25 (1988) 141–148.
[13] R.N. Chandler, D. Linton-Johnson, The equivalence of quasi-static flow in fluid-saturated porous media and the Biot's slow wave in the limit of zero frequency, J. Appl. Phys. 52 (1981) 3391–3395.
[14] D. Linton-Johnson, T. Plona, C. Scala, F. Pasieb, H. Kojima, Tortuosity and acoustic slow waves, Phys. Rev. Lett. 49 (1982) 1840–1844.
[15] D. Linton-Johnson, J. Koplik, L.M. Schwartz, New pore-size parameter characterizing transport in porous media, Phys. Rev. Lett. 57 (1986) 2564–2567.
[16] P. Nagy, L. Adler, Slow wave propagation in air-filled porous materials and in natural rocks, Appl. Phys. Lett. 56 (1990) 2504–2506.
[17] T. Schlief, J. Gross, J. Fricke, Ultrasonic attenuation in silica aerogels, J. Non-Cryst. Solids 145 (1992) 223–226.
[18] J. Stor-Pellinen, E. Haeggström, M. Luukkala, Measurement of paper-wetting processes by ultrasound transmission, Meas. Sci. Technol. 1 (2000) 406–411.
[19] P.L. Ridgway, A.J. Hunt, M. Quinby-Hunt, R.E. Russo, Laser ultrasonics on moving paper, Ultrasonics 37 (1999) 395–403.
[20] F. Montero, T.E. Gómez Álvarez-Arenas, A. Albareda, R. Pérez, J.A. Casals, High sensitivity piezoelectric transducers for NDE airborne applications, in: Proceedings of the Symposium on IEEE Ultrasonics, IEEE, New York, 2000, pp. 1073–1076.
[21] T.E. Gómez Álvarez-Arenas, F. Montero, Materiales y técnicas para el acoplamiento mecánico óptimo de piezocerámicas al aire, Bol. Soc. Esp. Cerám. Vidrio 41 (2002) 16–21.
[22] T.E. Gómez Álvarez-Arenas, B. González, F. Montero, Paper characterization by measurement of thickness and plate resonances using air-coupled ultrasound, in: Proceedings of the Symposium on IEEE Ultrasonics, IEEE, New York, 2002, in press.
[23] M. Luukkala, P. Heikkila, J. Surakka, Plate wave resonance, a contactless test method, Ultrasonics 9 (1971) 201–208.
[24] M. Khoury, G.E. Tourtollet, A. Schröder, Contactless measurement of the elastic Young's modulus of paper by an ultrasonic technique, Ultrasonics 37 (1999) 133–139.
[25] T.E. Gómez Álvarez-Arenas, F. Montero, Bridging the gap of impedance mismatch between air and solid materials, in: Proceedings of the Symposium on IEEE Ultrasonics, IEEE, New York, 2000, pp. 1069–1072.
[26] C.M. Fortunko, M.C. Renken, A. Murray, Examination of objects made of wood using air-coupled ultrasound, in: Proceedings of the Symposium on IEEE Ultrasonics, IEEE, New York, 1990, pp. 1099–1103.
[27] T.E. Gómez Álvarez-Arenas, F. Montero, M. Moner-Girona, E. Rodriguez, A. Roig, E. Molins, Viscoelasticity of silica aerogels at ultrasonic frequencies, Appl. Phys. Lett. 81 (7) (2002) 1198–1200.
[28] L. Flax, G.C. Gaunaurd, H. Überall, Theory of resonance scattering, in: W.P. Mason, R.N. Thurston (Eds.), Physical Acoustics, vol. 15, Academic Press, New York, 1981.
[29] L.M. Brekhovskikh, Waves in Layered Media, Academic Press, New York, 1960.
[30] R. Truell, Ch. Elbaum, B.B. Chick, Ultrasonic Methods in Solid State Physics, Academic Press, New York, 1969.
[31] S. Temkin, Elements of Acoustics, Wiley, New York, 1981.
[32] M.A. Biot, Theory of propagation of elastic waves in a fluid-saturated porous solid. I. Low-frequency range, J. Acoust. Soc. Am. 28 (1956) 168–178.
[33] M.A. Biot, Theory of propagation of elastic waves in a fluid-saturated porous solid. II. Higher frequency range, J. Acoust. Soc. Am. 28 (1956) 179–191.
[34] K. Wu, Q. Xue, L. Adler, Reflection and transmission of elastic waves from a fluid-saturated porous solid boundary, J. Acoust. Soc. Am. 87 (6) (1990) 2349–2358.
[35] S. Feng, D. Linton-Johnson, High-frequency acoustic properties of a fluid/porous solid interface, J. Acoust. Soc. Am. 74 (3) (1983) 906–914.
[36] T.E. Gómez Álvarez-Arenas, E. Riera, The generation of the Biot's slow wave at a fluid–porous solid interface. The influence of impedance mismatch, J. Phys. III 4 (C5) (1994) 187–190.
[37] T.E. Gómez Álvarez-Arenas, T. Montero, E. Molins, M. Moner-Girona, A. Roig, J.R. Rodriguez, S. Vargas, M. Esteves, Low-impedance and low-loss customized materials for air-coupled piezoelectric transducers, in: Proceedings of the Symposium on IEEE Ultrasonics, IEEE, New York, 2001, pp. 1077–1080.
[38] J. Fricke, T. Tillotson, Aerogels: production, characterization, and application, Thin Solid Films 297 (1997) 212–223.
[39] T.E. Gómez Álvarez-Arenas, L. Elvira, E. Riera, Generation of the slow wave to characterize air-filled porous fabrics, J. Appl. Phys. 78 (1995) 2843–2845.
[40] D. Linton-Johnson, T.J. Plona, Acoustic slow wave and the consolidation transition, J. Acoust. Soc. Am. 72 (1982) 556–565.
[41] S. Sundaram, J.D. Brantley, G. Howard Jr., H. Brandwein, Considerations in using "Bubble point" type tests as filter

integrity tests. Part I, Pharm. Technol. 24 (9) (2000) 90–115.
[42] P.R. Johnston, R.C. Lukaszwicz, T.H. Meltzer, Certain imprecisions in the bubble point measurement, J. Parenter. Sci. Technol. 35 (1981) 36–39.
[43] S. Sundaram, J.D. Brantley, G. Howard Jr., H. Brandwein, Considerations in using "Bubble point" type tests as filter integrity tests. Part II, Pharm. Technol. 24 (10) (2000) 108–137.
[44] S.P. Kelly, R. Farlow, G. Hayward, Applications of through-air ultrasound for rapid NDE scanning in the aerospace industry, IEEE Trans. Ultrason. Ferroelectr. Freq. Control 43 (1996) 581–591.